Molecular Therapy
Nucleic Acids
Original Article

Branchpoints as potential targets of exon-skipping therapies for genetic disorders

Hiroaki Ohara,[1,2,3,4] Motoyasu Hosokawa,[1,7] Tomonari Awaya,[1,5] Atsuko Hagiwara,[1] Ryo Kurosawa,[1] Yukiya Sako,[1,8] Megumu Ogawa,[3] Masashi Ogasawara,[3] Satoru Noguchi,[3] Yuichi Goto,[6] Ryosuke Takahashi,[2] Ichizo Nishino,[3] and Masatoshi Hagiwara[1]

[1]Department of Anatomy and Developmental Biology, Graduate School of Medicine, Kyoto University, Kyoto 606-8501, Japan; [2]Department of Neurology, Graduate School of Medicine, Kyoto University, Kyoto 606-8507, Japan; [3]Department of Neuromuscular Research, National Institute of Neuroscience, National Center of Neurology and Psychiatry, Tokyo 187-8502, Japan; [4]Department of Drug Discovery for Intractable Diseases, Graduate School of Medicine, Kyoto University, Kyoto 606-8501, Japan; [5]Laboratory of Tumor Microenvironment and Immunity, Graduate School of Medicine, Kyoto University, Kyoto 606-8501, Japan; [6]Department of Mental Retardation and Birth Defect Research, National Institute of Neurology, National Center of Neurology and Psychiatry, Tokyo 187-8502, Japan

Fukutin (*FKTN*) c.647+2084G>T creates a pseudo-exon with a premature stop codon, which causes Fukuyama congenital muscular dystrophy (FCMD). We aimed to ameliorate aberrant splicing of *FKTN* caused by this variant. We screened compounds focusing on splicing regulation using the c.647+2084G>T splicing reporter and discovered that the branchpoint, which is essential for splicing reactions, could be a potential therapeutic target. To confirm the effectiveness of branchpoints as targets for exon skipping, we designed branchpoint-targeted antisense oligonucleotides (BP-AONs). This restored normal *FKTN* mRNA and protein production in FCMD patient myotubes. We identified a functional BP by detecting splicing intermediates and creating BP mutations in the *FKTN* reporter gene; this BP was non-redundant and sufficiently blocked by BP-AONs. Next, a BP-AON was designed for a different FCMD-causing variant, which induces pathogenic exon trapping by a common SINE-VNTR-Alu-type retrotransposon. Notably, this BP-AON also restored normal *FKTN* mRNA and protein production in FCMD patient myotubes. Our findings suggest that BPs could be potential targets in exon-skipping therapeutic strategies for genetic disorders.

INTRODUCTION

Pseudo-exons are insertions of intronic sequences that are misrecognized as exons by deep intronic genetic variations. These can disrupt gene products via abnormal amino acid insertion or premature termination and may cause diseases.[1] However, the remaining coding sequences are preserved, and the full-length normal gene products can be restored when the pseudo-exons are repressed. Recently, such pseudo-exon-type mutations have been reported in many cases of neuromuscular disorders, including Fukuyama congenital muscular dystrophy (FCMD, OMIM: # 253800).[2]

FCMD is an intractable genetic disease characterized by severe dystrophic muscle wasting from birth or early infancy caused by biallelic defects of the *FKTN* gene.[3] Because of loss of ribitol-5-phosphate transferase encoded by *FKTN*,[4] patients with FCMD lack glycosylated forms of α-dystroglycan (α-DG) and are described as having α-dystroglycanopathy.[5] The deep intronic point mutation c.647+2084G>T (ClinVar: VCV000496331.7) creates a new splicing donor site in intron 5 and causes aberrant splicing to include a 64-bp pseudo-exon, which results in a frameshift and premature termination codon formation, leading to severe FCMD.[6,7]

We have been attempting to treat genetic disorders caused by pseudo-exons using small-molecule compounds with exon-skipping activity. Exons are defined by at least three essential splicing elements (5′ splice site, 3′ splice site, and branchpoint), which are recognized by U1 small nuclear ribonucleoprotein particles (snRNPs),[8] U2 snRNP auxiliary factor (U2AF),[9] and U2 snRNP,[10] respectively. Exons are further determined by additional splicing regulators, such as exonic and intronic splicing enhancers (ESEs and ISEs, respectively) and exonic and intronic splicing silencers (ESSs and ISSs, respectively). These regulators are recognized by serine/arginine-rich (SR) proteins, which positively regulate exon recognition, and heterogeneous nuclear ribonucleoproteins (hnRNPs), which negatively regulate exon recognition.[11] In principle, exon skipping can be achieved by inhibiting essential splicing elements or ESEs/ISEs. Genes with repetitive elements or unwanted exons, such as pseudo-exons, are good targets for exon skipping as a therapeutic strategy to recover full or partial gene products. Exon-skipping therapeutics using antisense oligonucleotides (AON) have already been approved in the US and Japan

Received 3 February 2023; accepted 11 July 2023;
https://doi.org/10.1016/j.omtn.2023.07.011.

[7]Present address: Department of Developmental Biology and Functional Genomics, Ehime University Graduate School of Medicine, Ehime 791-0295, Japan

[8]Present address: Moores Cancer Center, University of California, San Diego, La Jolla, CA 92093, USA

Correspondence: Tomonari Awaya, Department of Anatomy and Developmental Biology, Graduate School of Medicine, Kyoto University, Kyoto 606-8501, Japan.
E-mail: awaya@kuhp.kyoto-u.ac.jp
Correspondence: Masatoshi Hagiwara, Department of Anatomy and Developmental Biology, Graduate School of Medicine, Kyoto University, Kyoto 606-8501, Japan.
E-mail: hagiwara.masatoshi.8c@kyoto-u.ac.jp

 © 2023 The Authors.
This is an open access article under the CC BY-NC-ND license (http://creativecommons.org/licenses/by-nc-nd/4.0/).

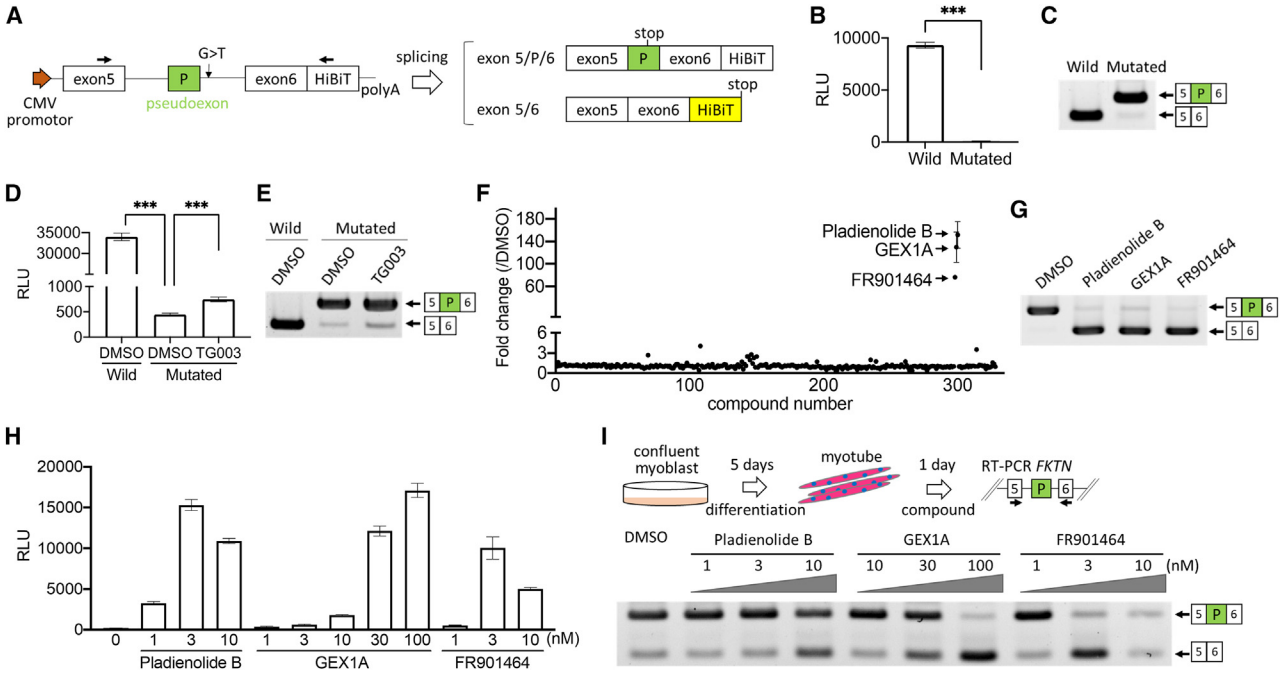

Figure 1. Identification of SF3B1 inhibitors as potent agents for suppressing the c.647+2084G>T-induced pseudo-exon of *FKTN*

(A) Diagram of the *FKTN* splicing reporter, *FKTN* minigene of exon 5–6 with intron 5 (wild type), or exon 5–6 with c.647+2084G>T-harboring intron 5 (mutated type) with a HiBiT tag. Filled arrows indicate primers for RT-PCR. (B and C) HEK293 cells were transfected with the wild-type or mutated reporter for 24 h. The luminescence value was quantified by relative luminescence units (RLUs) generated by the C-terminal HiBiT tag using the Nano-Glo HiBiT Lytic Detection System (B). Pseudo-exon expression was confirmed using RT-PCR (C). The larger band corresponds to the 64-bp pseudo-exon inclusion between exons 5 and 6. (D and E) HEK293 cells were transfected with the wild-type or mutated reporter for 4 h and treated with TG003 (30 μM) or DMSO for 24 h. DMSO was used as a negative control because it was used as a solvent for the compounds. The effect of TG003 was confirmed by HiBiT assay (D) and RT-PCR (E). The NanoLuc luciferase activity of TG003 was 1.7-fold higher than that of DMSO. (F) Scatterplot of the fold change of RLUs using the *FKTN* splicing reporter in focused library screening. (G) RT-PCR analysis of the *FKTN* splicing reporter with SF3B1 inhibitors (10 μM) and DMSO in HEK293 cells after 24 h. (H) HiBiT assay using the *FKTN* splicing reporter with pladienolide B (1–10 nM), GEX1A (1–100 nM), and FR901464 (1–10 nM). (I) SF3B1 inhibitor effect in patient-derived myotubes with the *FKTN* c.647+2084G>T mutation. RT-PCR analysis was performed using pladienolide B (1, 3, or 10 nM), GEX1A (10, 30, or 100 nM), FR901464 (1, 3, or 10 nM), or DMSO. Filled arrows indicate primers for RT-PCR. Data are shown as mean ± SD (n = 4). ***$p < 0.001$, calculated by t test using Welch's two-sample t test.

to treat Duchenne muscular dystrophy and are intensively investigated for other diseases.[12]

We have achieved promotion of exon skipping using small-molecule inhibitors of CDC-like kinases (CLKs), which inactivate SR proteins by inhibiting serine phosphorylation in their carboxy-terminal arginine/serine-rich domain in disease models of cystic fibrosis (caused by *CFTR* c.3718-2477C>T),[13] Duchenne muscular dystrophy (caused by *DMD* c.4303G>T),[14,15] and anhidrotic ectodermal dysplasia with immunodeficiency (caused by *IKBKG* c.518+866C>T).[16] In addition, small-molecule compounds inhibiting splicing factor 3b (SF3b) complex, which is a major component of U2 snRNPs, are known to induce exon skipping.[17] To determine the best exon skipping strategy for the pseudo-exon caused by the *FKTN* c.647+2084G>T mutation, we created a high-sensitivity luminescent splicing reporter and screened our custom compound library with a focus on RNA splicing regulation. Here, we discovered that the branchpoint could be a potential therapeutic target. We designed branchpoint-targeted AONs (BP-AONs) and confirmed the effectiveness of BPs as targets for exon skipping.

RESULTS

Generation of the *FKTN* splicing reporter system

We constructed novel splicing reporters to analyze the splicing pattern of the pseudo-exon created by *FKTN* c.648+2084G>T variation, screened compounds, and recapitulated the abnormal splicing pattern in an efficient and highly quantitative manner. *FKTN* gene fragments, including exons 5 and 6 with intron 5 in between, harboring either the G (wild-type) or the T (mutant) allele in intron 5, were fused in frame with a HiBiT tag, which emits bright luminescence upon incubation with LgBiT fragments and substrates (Figure 1A). In this system, the normal splicing reporter (skipping the pseudo-exon in intron 5) exhibited high NanoLuc luciferase activity, whereas the pathogenic splicing reporter (including the pseudo-exon) did not (Figure 1B). This difference between pathogenic and wild-type splicing reporters was considered adequate for screening compounds (z' factor = 0.90). The consistency of the *FKTN* splicing reporter was confirmed by RT-PCR. The larger band corresponding to the pseudo-exon inclusion was dominantly expressed in the mutated-type reporter, which was consistent with previously reported

findings (Figure 1C).[6,7] Using this splicing reporter system, we then examined the effect of TG003, a CLK inhibitor, which has been reported previously as an exon-skipping agent.[14,16,18] NanoLuc luciferase activity was 1.7-fold higher with TG003 treatment than with DMSO (Figure 1D). The exon-skipping effect of TG003 was confirmed by RT-PCR and was consistent with the HiBiT assay results (Figure 1E). The results confirmed that our HiBiT reporter system sensitively recaptured the amount of pseudo-exon skipping in the presence of TG003; thus, we moved on to compound screening using this system.

SF3B1 inhibitors were identified as highly potent rectifiers of aberrant splicing

To explore small-molecule compounds that induce pseudo-exon skipping of *FKTN* mRNA, we screened 327 compounds from a customized compound library focused on chemicals targeting splicing-regulatory elements and found three SF3B1 inhibitors to be highly potent candidates that could restore the normal splicing product. Our library consisted of our original chemicals and commercially available compounds, including SR protein kinase inhibitors, such as CLK and SR protein kinase (SRPK) inhibitors; splicing modulators, such as RECTAS[19]; SF3B1 inhibitors and RNA binding motif 39 (RBM39) degraders; and TG003 as a positive control (Table S1). We found that CLK inhibitors with a structure similar to TG003 showed 3- to 5-fold higher relative light units (RLUs) compared with that of DMSO. Moreover, we found extremely high RLUs (80- to 150-fold) in pladienolide B-,[20] GEX1A-,[21] and FR901464-treated cells (Figure 1F),[22] all of which were classified as SF3B1 inhibitors. In addition, we performed a 2-(2-methoxy-4-nitrophenyl)-3-(4-nitrophenyl)-5-(2,4-disulfo-phenyl)-2H-tetrazolium, monosodium salt (WST-8) cell proliferation assay to assess cytotoxicity. We found that RLUs in TG003, pladienolide B, GEX1A, and FR901464 showed 0.76-fold, 0.74-fold, 0.67-fold, and 0.70-fold changes, respectively, compared with DMSO (Figure S1). These results demonstrated that SF3B1 inhibitors did not significantly affect cell viability at this concentration.

The effects of these compounds were confirmed by RT-PCR (Figure 1G). The dose-dependent effects of these compounds were evaluated. The luminescence values of pladienolide B, GEX1A, and FR901464 gradually increased to 68.7-fold at 3 nM, 76.8-fold at 100 nM, and 45.1-fold at 3 nM, respectively, compared with the DMSO control (Figure 1H).

To evaluate the efficacy of pseudo-exon skipping under more physiological conditions, we cultured myotubes from patient-derived myoblasts carrying the c.647+2084G>T variant of the *FKTN* gene (G>T myotubes) (Figure 1I). We confirmed a 64-bp pseudo-exon insertion between exons 5 and 6 in *FKTN* mRNA from G>T-myotubes by RT-PCR and direct sequencing (data not shown) and then examined the effect of SF3B1 inhibitors on *FKTN* pseudo-exon skipping. Similar to the *FKTN* splicing reporter results, SF3B1 inhibitors induced *FKTN* pseudo-exon skipping and restored the normal splicing pattern in *FKTN* mRNA exons 5 and 6 (Figure 1I).

SF3B1 inhibitors induce multiple exon-skipping in G>T myotubes

SF3B1 inhibitors directly interfere with the interaction between pre-mRNA and the U2snRNP complex and have global effects on splicing in a time- and dose-dependent manner, resulting in dramatic alterations in transcriptional dynamics.[17,20,23] RT-PCR result showed that the band intensities of the inclusion and skipped forms at the 10-nM dose of FR901464 were faint compared with those at the 3-nM dose in G>T myotubes (Figure 1I). This indicated that higher doses of FR901464 reduced total transcripts, reflecting global splicing alteration. Therefore, we assessed the splicing patterns of other exons in the *FKTN* gene in myotubes to check the effect of SF3B1 inhibitors by RT-PCR with different primer sets. Several aberrantly spliced products were detected by RT-PCR of exons 5–10, such as skipping of exons 7, 8, and 9 in combination, in addition to pseudo-exon inclusion (Figure 2A). Because SF3B1 inhibitors induce skipping of exons other than the pseudo-exon at high concentrations, SF3B1 inhibitors have limited therapeutic windows for treating the *FKTN* c.647+2084G>T variant, although BP inhibition was found to be effective for pseudo-exon skipping. Therefore, we designed AONs specifically targeting the BP upstream of the pseudo-exon.

AON#1 and AON#2 restored correct splicing of the mutant allele and increased glycosylated α-DG expression in G>T myotubes

BPs are generally located within 18–50 nt upstream of the 3′ splice site (hereafter called "BP window") and are mostly adenines.[24,25] To search for promising target sequences, we designed three different AONs that covered all adenines located in the BP window upstream of the pseudo-exon (Figure 2B). We transfected patient-derived myoblasts with AON#1, AON#2, and AON#3 at two concentrations (30 and 100 nM) and differentiated them into myotubes for 4 days. AON#1 and AON#2 skipped pseudo-exons in 5-P-6-7-8-9-10 and 5-P-6-10 isoforms in a dose-dependent manner and increased 5-6-7-8-9-10 and 5-6-10 skipped isoforms, respectively, indicating that AON#1 and AON#2 skipped the pseudo-exons without affecting other exon composition (Figure 2C). The spliced ratios (full length/total isoform) of AON#1 and AON#2 gradually increased to 0.63 and 0.53 at 100 nM. Next, we tried to assess whether AON#1 could restore functional FKTN protein, but we could not detect FKTN protein with commercially available anti-FKTN antibodies. Instead, we used α-DG glycosylation, a hallmark of FCMD pathomechanisms, as a surrogate marker to confirm the possible therapeutic effect of AON#1. We used myoblasts from a congenital myopathy patient (CMP) without abnormal *FKTN* as a reference. Western blotting showed an increase in glycosylated α-DG protein compared with the mock control (Figure 2D). Immunofluorescence staining also showed an immense increase in glycosylated α-DG levels (Figure 2E), indicating that BP-AONs restored functional FKTN levels.

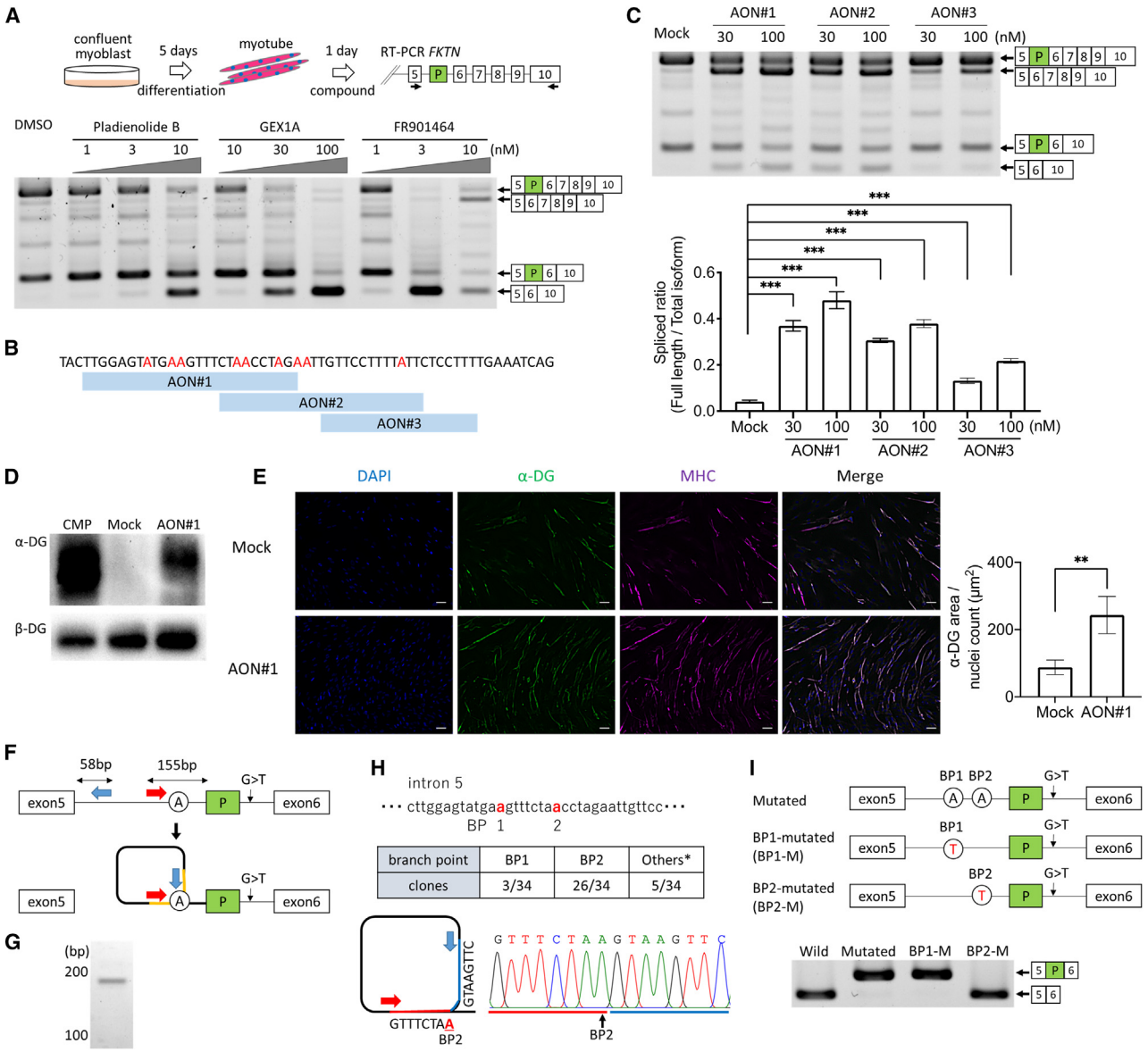

Figure 2. BP-AON induced pseudo-exon skipping of *FKTN* mRNA

(A) RT-PCR analysis for *FKTN* exons 5–10 in patient-derived myotubes with a c.647+2084G>T in the presence of SF3B1 inhibitors. Filled arrows indicate primers for RT-PCR. (B) AON design targeting BPs upstream of the pseudo-exon. Adenines located within the 18- 50-nt window from the pseudo-exon are colored red. (C) RT-PCR analysis was performed with AON#1, AON#2, AON#3 (30 or 100 nM), or mock. The full length (FL)/total splice ratio was quantified using intensity analysis. (D) Western blotting of glycosylated α-dystroglycan (α-DG) in patient-derived myotubes treated with AON#1 (100 nM) or mock. β-Dystroglycan (β-DG) was used as a loading control. (E) Patient-derived myotubes showing α-DG glycosylation (clone IIH6, green) and myosin heavy chain (clone MF20, magenta) after treatment with AON#1 (100 nM) or mock. Scale bars, 50 μm. (F) Schematic of divergent primers for lariat introns in the *FKTN* splicing reporter upstream of the pseudo-exon, where "A" denotes the BP. RT-PCR detected branched structures of introns (yellow). (G) RT-PCR results for the lariat intron. (H) BPs were detected using TA cloning and Sanger sequencing. The main BP, BP2, the adenine located 38 bp from the pseudo-exon, is shown selectively. (I) Diagram showing *FKTN*-mutated, BP1-mutated (BP1-M), and BP2-mutated (BP2-M) reporters. RT-PCR analysis revealed skipping of the pseudo-exon in BP2-M. Data represent the mean ± SD (n = 4). $^{**}p < 0.01$ and $^{***}p < 0.001$, calculated using Welch's two-sample t test or one-way ANOVA with independent post hoc Tukey's multiple-comparisons test.

Identification of BPs from lariat introns

Given that AON#1 and AON#2 were more effective than AON#3, we mapped which adenines were actually used for a BP in inclusion of this pseudo-exon. We performed RT-PCR for the lariat intron and sequenced RT-PCR products derived from the reporter. We designed divergent primers upstream of the pseudo-exon to detect lariat introns across BPs (Figure 2F) and successfully detected RT-PCR products of the expected size (Figure 2G). The

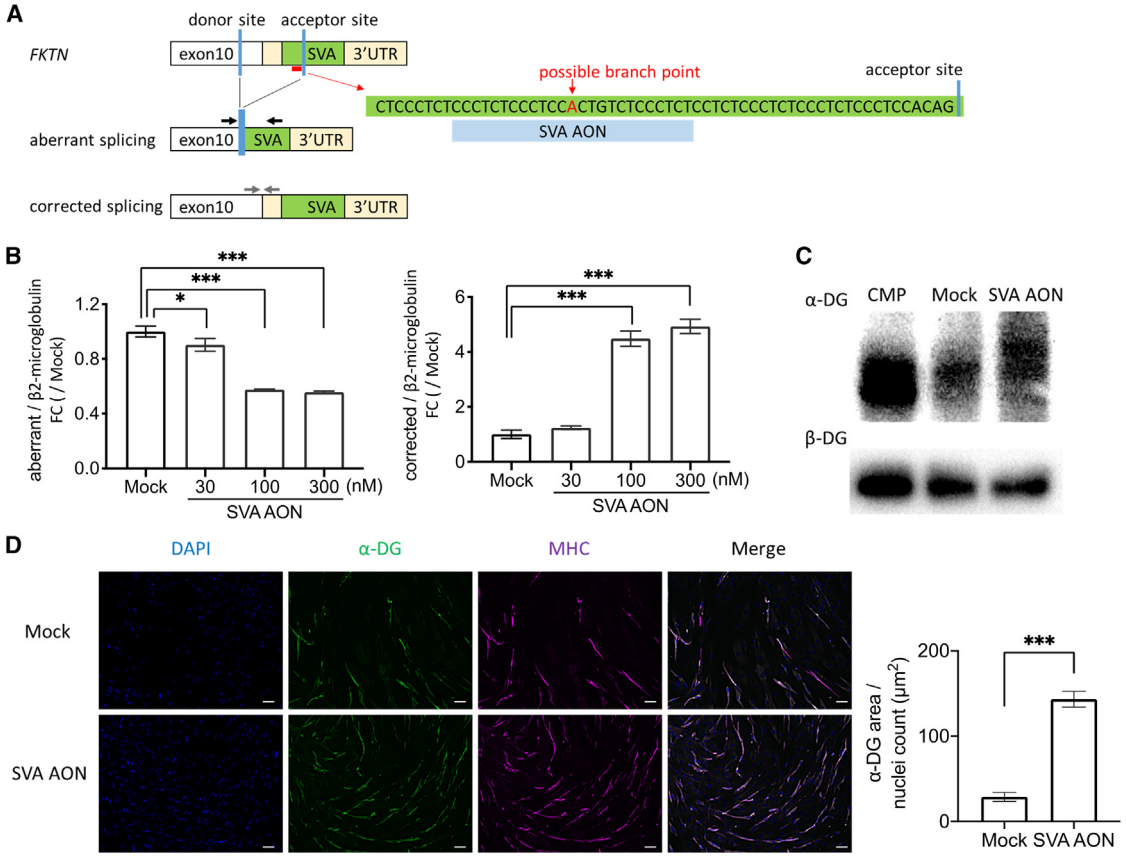

Figure 3. BP-AON effect in myotubes derived from a patient with FCMD with homozygous SVA retrotransposon insertions

(A) Representation of abnormal splicing in *FKTN* with SVA retrotransposon insertions and AON design targeting one possible non-redundant BP (SVA-AON). Shown is a schematic of primers for abnormal RT-PCR products (black arrow) and corrected RT-PCR products (gray arrow). (B) qRT-PCR of aberrant splicing and corrected splicing in myotubes treated with SVA-AON (30, 100, or 300 nM) or mock. β2-Microglobulin was used as an internal control. Data are shown as mean ± SD (n = 3). (C) Western blot of glycosylated α-DG treated with SVA-AON (100 nM) or mock. β-DG was used as a loading control. (D) Patient-derived myotubes showing α-DG glycosylation (clone IIH6, green) and myosin heavy chain (clone MF20, magenta) after treatment with SVA-AON (100 nM) or mock. Scale bars, 50 μm. Data represent the mean ± SD (n = 4). *$p < 0.05$, **$p < 0.01$, and ***$p < 0.001$, calculated using Welch's two-sample t test or one-way ANOVA with independent post hoc Tukey's multiple-comparisons test.

PCR products were cloned into TA cloning vectors to sequence a total of 34 TA clones (Figure 2H). Three clones (9%) used an adenine located 46 bp from the pseudo-exon (BP1; c.647+1969A), and 26 clones (76%) used an adenine located 38 bp from the pseudo-exon (BP2; c.647+1977A) as a BP. The remaining five clones (15%) were BPs induced by cryptic 5′ splice sites. These results demonstrated that BP2 was predominantly used for pseudo-exon inclusion induced by the c.647+2084G>T variant in the splicing reporter.

BPs are weakly conserved, and BP multiplicity or redundancy occurs frequently.[26] To determine whether BP2 destruction results in pseudo-exon skipping, we created a BP1- and BP2-mutated reporter (BP1-M and BP2-M, respectively) by replacing the adenine with a thymidine (c.647+1969A>T and c.647+1977A>T) in the mutated reporter (Figure 2I). The A-to-T substitution at BP2 completely suppressed the pseudo-exon, whereas that at BP1 did not. These results indicate that the *FKTN* pseudo-exon is highly dependent on BP2. This was consistent with the result that AON#1 and AON#2 had a stronger effect than AON#3 because BP2 was covered by AON#1 and AON#2 but not by AON#3.

Design of a BP-AON against FCMD with homozygous SINE-VNTR-Alu retrotransposon insertions

To further evaluate whether BP-AONs could be applied to other mutations, we designed a BP-AON for the SINE-VNTR-Alu (SVA)-type retrotransposon insertion mutation in FCMD, which induces aberrant splicing by SVA exon trapping.[27] There was only one adenine located within the BP window from the cryptic acceptor site. Hence, we designed an AON-targeting adenine (SVA-AON) (Figure 3A).

SVA-AON also rectifies aberrant splicing and glycosylation of α-DG in patient-derived myotubes with homozygous SVA retrotransposon insertions

We transfected confluent patient-derived myoblasts with homozygous SVA retrotransposon insertions using SVA-AON at different

concentrations (30, 100, or 300 nM) and differentiated them into myotubes for 4 days. Quantitative reverse-transcriptase PCR (qRT-PCR) showed that SVA-AON suppressed aberrant splicing in a dose-dependent manner by up to 56% and increased the number of correctly spliced transcripts by 493% at 300 nM (Figure 3B). Western blotting of glycosylated α-DG showed a significant shift toward a higher molecular weight compared with the mock control, indicating successful functional restoration of the FKTN protein (Figure 3C). Immunofluorescence staining also showed an immense increase in glycosylated α-DG levels (Figure 3D). These results demonstrated that the BP-targeting strategy also worked for the SVA-type *FKTN* variant.

DISCUSSION

In this study, we demonstrated that BPs could be potential targets for exon-skipping therapeutic strategies to treat genetic disorders. This report presents the first successful case of splicing correction by AON-based targeting of BPs. We identified SF3B1 inhibitors as highly effective compounds that promoted pseudo-exon skipping. The effect of SF3B1 inhibitors was much higher than that of other splicing modification compounds, including our own CLK inhibitors, and SF3B1 inhibitors skipped the pseudo-exon in *FKTN* G>T myotubes. However, higher concentrations of SF3B1 inhibitors skipped not only the pseudo-exon but also other exons, resulting in degradation of *FKTN* mRNA. Thus, we designed the AON to block the BP specifically.

BP motifs are variable and redundant[26] and have not been considered good targets for exon-skipping AONs. We hypothesized that, if we could determine and block functioning BPs with AONs, then we could efficiently skip pseudo-exons. We performed several experiments to determine a functional BP from adenine residues that could be used as BPs and discovered that BP2 of the *FKTN* pseudo-exon was the only BP actually used and that nucleotide substitution of BP2 completely skipped the pseudo-exon. These observations indicated that the pseudo-exon depended on a single functional BP, BP2, which was the reason why only AON#1 and AON#2 efficiently skipped the pseudo-exon. For abnormal splicing caused by SVA-type retrotransposon insertions in the 3′ UTR, there was only one adenine that could be used as a BP. SVA-AON covered the adenine and sufficiently inhibited the abnormal exon trapping caused by the SVA insertions.

Determination of functional BPs is important, and their inhibition may lead to effective exon skipping. Recent progress in computational technologies has enabled us to predict BPs.[28] For the *FKTN* c.647+2084G>T variant, SVM-BPfinder[25] and RNABPS (RNA Branch Point Selection)[29] predicted BP2 as a BP with high probability, which was consistent with our results. As the accuracy of such prediction programs improves, they can also be used in AON design in the future.

Recently, several AONs to treat Duchenne muscular dystrophy (DMD) have been approved and are clinically available in several countries.[30–33] AONs for exon skipping, including those currently under development, target ESEs or splice sites, and no AONs target BPs.[12] However, there are several potential advantages to targeting BP. First, BP-AONs can be highly specific because BP motifs are degenerated and diverse. In RNA sequencing (RNA-seq) analysis, intronic off-target sites have been reported to be much fewer than off-target sites detected within exons.[34] Second, it is relatively easy to design AONs targeting BPs compared with those targeting ESEs or splice sites. The current major approach is AON walking, which creates dozens of AONs that cover all possible splicing-regulatory elements around exons overlapping each other. For example, in NS-065/NCNP-01, an AON for DMD, 38 AONs were designed in the first screening.[35] Because BPs are usually located within nucleotides 18–50 bases upstream of a 3′ splice site,[24,25] and the residue is adenine, we can easily find possible BPs to use for the target exon.

In the case of the *FKTN* c.647 + 2084G>T mutation, the screened compounds were not suitable for therapeutic use. However, we found that the BP is a good target for exon skipping. Splicing modulator screening is an effective way to determine which splicing-regulatory elements are engaged in exon recognition and should be inhibited to induce efficient exon skipping. When SF3B1 inhibitors are effective in compound screening, determination of the functional BP will enable us to design BP-AONs that are appropriate and efficient for exon skipping.

In summary, our findings suggested that the splicing BPs, which have been largely ignored as treatment targets, may be appropriate targets for exon skipping. Our novel AON design strategy will help us develop new AON-based therapeutics for many genetic disorders.

MATERIALS AND METHODS

Patients

Three patients in this study provided written informed consent for muscle biopsy samples following the Declaration of Helsinki protocols. Myoblast cultures from three patients were obtained from muscle biopsies. The establishment and use of patient myoblasts were approved by the institutional ethics committee of National Center of Neurology and Psychiatry, and Kyoto University Graduate School of Medicine.

Compounds

TG003 was prepared as described previously.[18] Briefly, TG003 was dissolved in DMSO (Sigma-Aldrich, St. Louis, MO, USA). Some compound libraries were provided by the Medical Research Support Center, Kyoto University Graduate School of Medicine. FR901464 (catalog number A12702) was purchased from Adooq Biosciences (Irvine, CA, USA). Pladienolide B (catalog number sc-391691) was purchased from Santa Cruz Biotechnology (Santa Cruz, CA, USA). GEX1A (catalog number 25136) was purchased from Cayman Chemical (Ann Arbor, MI, USA). The compounds were dissolved in DMSO at 50 mM, with the exception of FR901464, pladienolide B, and GEX1A, which were dissolved at 1 mM. All compounds were kept at −80°C.

Cell culture

HEK293 cells (human embryonic kidney cells; American Type Culture Collection, Manassas, VA, USA) were maintained in high-glucose Dulbecco's modified Eagle's medium (Nacalai Tesque, Kyoto, Japan) supplemented with 10% fetal bovine serum (Sigma-Aldrich), 100 units/mL penicillin, and 100 mg/mL streptomycin (Nacalai Tesque). Myoblasts were maintained in Dulbecco's modified Eagle's medium/nutrient mixture F-12 medium (Thermo Fisher Scientific, Waltham, MA, USA) supplemented with 20% fetal bovine serum (Sigma-Aldrich), 100 units/mL penicillin, and 100 mg/mL streptomycin (Nacalai Tesque). Myotubes were obtained from confluent myoblast cultures after 4–7 days of serum deprivation and replacement with 5% horse serum (Thermo Fisher Scientific). The cells were grown at 37°C with 5% CO_2 under humid conditions in a tissue culture incubator.

Reporter construction

We constructed *FKTN* splicing reporters as described in Figure 1A. A human *FKTN* genomic DNA fragment spanning exons 5–6 with or without a mutation of c.647+2084G>T with a carboxyl-terminal HiBiT tag was synthesized by Eurofins Genomics (Tokyo, Japan) and cloned into pcDNA3.1. The HiBiT sequence was provided by Promega (Madison, WI, USA). BP2-mutated cells were introduced using a PCR-based method[36] on the pGEM-T Easy vector (Promega).

HiBiT assay, cell viability assay, and transfection

For the HiBiT assay, HEK293 cells (4.0×10^6 cells in a 10-cm dish) were transfected with the *FKTN* splicing reporter using FuGENE HD transfection reagent (Promega). Four hours after transfection, cells were seeded into a 96-well plate (5.0×10^4 cells/well) and incubated with compounds or DMSO (negative control) for 24 h. Luminescence was subsequently measured using the Nano Glo HiBiT Lytic Detection System according to the manufacturer's instructions (Promega). Cell viability was determined by the WST-8 Cell Proliferation Assay Kit (Nacalai Tesque). WST-8 was added to each well for 1 h before measurement, following the manufacturer's instructions. Three biological replicates were used for each assay.

RNA isolation and RT-PCR

Total RNA was isolated using the RNeasy Mini Kit (QIAGEN, Hilden, Germany), followed by DNase treatment, according to the manufacturer's instructions. Reverse transcription was conducted using PrimeScript reverse transcriptase (Takara Bio, Shiga, Japan) (HEK293 cells) or SuperScript IV reverse transcriptase (Thermo Fisher Scientific) (all myoblasts) and oligo(dT)20 primers or gene-specific primers (5′-CCA TTG GGT TGC ACA TTG GG-3′) (*FKTN*-mRNA of FCMD patient myoblasts with a mutation of c.647+2084G>T) and random hexamers (Takara Bio) (lariat introns in the *FKTN* splicing reporter), followed by PCR with Ex Taq polymerase (Takara Bio). The RT-PCR products were separated by electrophoresis. Ethidium bromide-stained images were captured using ChemiDoc (Bio-Rad, Hercules, CA, USA) and analyzed using the Image Lab software (Bio-Rad). The following primers were used for semi-quantitative RT-PCR: 5′-GCA CGG CCA CTT GAG ACT TA-3′ (forward primer of *FKTN* exon 5 for HEK293 cells), 5′- CGA AAT CTT CTT GAA CAG CCG CC-3′ (reverse primer of HiBiT for HEK293 cells), 5′-CGT TAT CCA GGA GCT TTT GAC AG-3′ (forward primer of *FKTN* exon 5 for myoblasts), 5′-TGC TCG AGC TTC TTT ATA CCT ACA-3′ (reverse primer of *FKTN* exon 6 for myoblasts), 5′-GCT TCC AGT CCC ACG TCT TT-3′ (reverse primer of *FKTN* exon 10 for myoblasts), 5′-GTG AGA AAC AGT TAT TTG AAG GAA C-3′ (forward primer for lariat introns in the *FKTN* splicing reporter), and 5′-CAA GAA TTA TGA CTG AAC AAC ACT CA-3′ (reverse primer for lariat introns in the *FKTN* splicing reporter).

qRT-PCR

qRT-PCR was performed using PowerUp SYBR Green Master Mix (Thermo Fisher Scientific) according to the manufacturer's protocol. The data were normalized to β2-microglobulin expression. The following primers were used for qRT-PCR: 5′-TGT ACC CTG TGA AAC CCT CG-3′ (forward primer for abnormal splicing in *FKTN* with SVA retrotransposon insertions), 5′-GAA AAC CAG TGA GGC GTA GC-3′ (reverse primer for abnormal splicing in *FKTN* with SVA retrotransposon insertions), 5′-GCA ACC CAA TGG AAT CTG GC-3′ (forward primer for corrected splicing in *FKTN* with SVA retrotransposon insertions), 5′-TGG TTC CCA CTT ATG TTT GAC A-3′ (reverse primer for corrected splicing in *FKTN* with SVA retrotransposon insertions), 5′-CCA CTG AAA AAG ATG AGT ATG CCT-3′ (forward primer for β2-microglobulin), and 5′-CCA ATC CAA ATG CGG CAT CTT CA-3′ (reverse primer for β2-microglobulin).

AON design and composition

AONs were designed to target the BP and synthesized in 2′-O-methyl phosphorothioate (Integrated DNA Technologies, Coralville, IA, USA) as follows: AON#1, 5′- CUAGGUUAGAAACUUCAUACUC CAA-3′; AON#2, 5′-AAUAAAAGGAACAAUUCUAGGUUAG-3′; AON#3, 5′-AAAGGAGAAUAAAAGGAACA-3′; SVA-AON, 5′-AG AGGGAGACAGUGGAGGGAGAGGG-3′. RNAiMaX (Thermo Fisher Scientific) was used as the transfection reagent in Opti-MEM (Thermo Fisher Scientific). For transfection, myoblasts were seeded in a 24-well plate (2.0×10^5 cells per well) or 10-cm dish (4.0×10^6 cells) in growth medium to reach 80%–100% confluence on the following day. Myoblasts were then transfected for 4 h according to the manufacturer's instructions and changed to differentiation medium for myotube differentiation.

Western blotting

For western blot analysis, myotubes were collected from a 10-cm dish in 200 μL lysis buffer (20 mM Tris [pH 8.0], 150 mM NaCl) containing 2% Triton X-100 and protease inhibitors, sonicated, and kept at 4°C for 2 h. Samples were spun down for 5 min at 10,000 rpm. The supernatant fluid was solubilized in 1.8 mL lysis buffer and incubated in 60 μL wheat germ agglutinin (WGA)-agarose (J-Chemical, Tokyo, Japan). The following day, the WGA beads were washed three times with 0.2% Triton in lysis buffer and heated to 95°C for 5 min with 60 μL of sample buffer (Nacalai Tesque). The samples were

electrophoresed on a 7.5% SuperSep Ace Gel (Wako Pure Chemicals Industries, Osaka, Japan) and transferred to polyvinylidene fluoride (PVDF) membranes (Pall, Port Washington, NY, USA). Antibody reactions were performed using Can Get Signal Immunoreaction Enhancer Solution (Toyobo, Osaka, Japan). Primary antibody incubation was performed at 4°C overnight, and secondary antibody incubation was performed at 25°C for 1 h. Peroxidase activity was visualized using ImmunoStar LD (Wako Pure Chemicals Industries) and a ChemiDoc MP Imaging System (Bio-Rad). The following antibodies were used for western blotting: mouse monoclonal anti-α-DG (VIA4-1; Merck Millipore, Darmstadt, Germany), mouse monoclonal anti-β-DG (43DAG1/8D5; Leica Biosystems, Buffalo Grove, IL, USA), and horseradish peroxidase (HRP)-conjugated anti-mouse immunoglobulin (IgG) goat polyclonal antibody as a secondary antibody (Abcam, Cambridge, UK).

Immunofluorescence

Cells were fixed in 4% paraformaldehyde for 15 min at 25°C. After washing with PBS, the cells were blocked with PBS containing 3% bovine serum albumin (Wako Pure Chemicals Industries) and 0.1% Triton X-100 for 1 h at 25°C. The cells were then incubated with primary antibodies at 4°C overnight. The primary antibodies used in this study were mouse monoclonal anti-α-DG (IIH6C4, Merck Millipore) and mouse monoclonal anti-myosin heavy chain (MF20, R&D Systems, Minneapolis, MN, USA). After washing twice with PBS, cells were incubated with secondary antibodies for 1 h at 25°C. The secondary antibodies used were goat polyclonal Alexa Fluor 488-conjugated anti-mouse IgM (Thermo Fisher Scientific) and goat polyclonal Alexa Fluor 647-conjugated anti-mouse IgG (Thermo Fisher Scientific). DAPI was used for nuclear staining. After staining, all samples were analyzed using a BZ-X710 fluorescence microscope (Keyence, Osaka, Japan) using BZ-X Analyzer software (Keyence).

Statistical analysis

Values are presented as mean ± SD. Statistical significance was evaluated with a two-tailed Student's or Welch's t test to analyze differences between two experimental groups ($p < 0.05$ was considered significant). In Figures 2C and 3B, statistical significance was evaluated with one-way ANOVA with independent post hoc Tukey's multiple-comparisons test ($p < 0.05$ was considered significant).

DATA AVAILABILITY STATEMENT

The data for this study are available from the corresponding author upon request.

SUPPLEMENTAL INFORMATION

Supplemental information can be found online at https://doi.org/10.1016/j.omtn.2023.07.011.

ACKNOWLEDGMENTS

We would like to thank the Kyoto University Medical Research Support Center for technical support. We also thank Dr. C. Tsuzuki for technical assistance, Dr. Y. Okuno and members of the M. Hagiwara laboratory at Kyoto University for helpful comments and technical advice, Editage (www.editage.jp) for English language editing, and Science Graphics (www.s-graphics.co.jp) for graphical abstract editing. This research was supported by JSPS KAKENHI grants JP15H05721 and JP21H05042 (to M. Hagiwara and T.A.), JP20K17509 (to M. Hosokawa), and JP22K20710 (to H.O.), Japan; JST START University Ecosystem Promotion Type (Supporting Creation of Startup Ecosystem in Startup Cities) grant JPMJST2181, Japan (to T.A.); AMED grants JP22gm4010013 (to M. Hagiwara) and JP22ek0109490h0003 (to S.N. and I.N.), Japan; and Intramural Research Grants for Neurological and Psychiatric Disorders of NCNP 2-5 (to I.N.), 2-6 (to S.N.), and 3-9 (to S.N). This research was also supported by BTB Drug Development Research Center Co., Ltd. and Torii Pharmaceutical Co., Ltd.

AUTHOR CONTRIBUTIONS

H.O., M. Hosokawa, and T.A. designed and conducted this study. H.O., M. Hosokawa, T.A., and M. Hagiwara wrote the manuscript. H.O., M. Hosokawa, A.H., Y.S., M. Ogawa, M. Ogasawara, and T.A. performed experiments. H.O., M. Hosokawa, R.K., and T.A. analyzed the data. R.T., S.N., Y.G., I.N., and M. Hagiwara supervised the study. All authors approved the final manuscript.

DECLARATION OF INTERESTS

The authors declare no competing interests.

REFERENCES

1. Vaz-Drago, R., Custódio, N., and Carmo-Fonseca, M. (2017). Deep intronic mutations and human disease. Hum. Genet. *136*, 1093–1111.
2. Okubo, M., Noguchi, S., Awaya, T., Hosokawa, M., Tsukui, N., Ogawa, M., Hayashi, S., Komaki, H., Mori-Yoshimura, M., Oya, Y., et al. (2023). RNA-seq analysis, targeted long-read sequencing and in silico prediction to unravel pathogenic intronic events and complicated splicing abnormalities in dystrophinopathy. Hum. Genet. *142*, 59–71.
3. Fukuyama, Y., Osawa, M., and Suzuki, H. (1981). Congenital progressive muscular dystrophy of the Fukuyama type - clinical, genetic and pathological considerations. Brain Dev. *3*, 1–29.
4. Kanagawa, M., Kobayashi, K., Tajiri, M., Manya, H., Kuga, A., Yamaguchi, Y., Akasaka-Manya, K., Furukawa, J.I., Mizuno, M., Kawakami, H., et al. (2016). Identification of a Post-translational Modification with Ribitol-Phosphate and Its Defect in Muscular Dystrophy. Cell Rep. *14*, 2209–2223.
5. Muntoni, F., Brockington, M., Blake, D.J., Torelli, S., and Brown, S.C. (2002). Defective glycosylation in muscular dystrophy. Lancet *360*, 1419–1421.
6. Lim, B.C., Ki, C.S., Kim, J.W., Cho, A., Kim, M.J., Hwang, H., Kim, K.J., Hwang, Y.S., Park, W.Y., Lim, Y.J., et al. (2010). Fukutin mutations in congenital muscular dystrophies with defective glycosylation of dystroglycan in Korea. Neuromuscul. Disord. *20*, 524–530.
7. Kobayashi, K., Kato, R., Kondo-Iida, E., Taniguchi-Ikeda, M., Osawa, M., Saito, K., and Toda, T. (2017). Deep-intronic variant of fukutin is the most prevalent point mutation of Fukuyama congenital muscular dystrophy in Japan. J. Hum. Genet. *62*, 945–948.
8. Mount, S.M., Pettersson, I., Hinterberger, M., Karmas, A., and Steitz, J.A. (1983). The U1 small nuclear RNA-protein complex selectively binds a 5' splice site *in vitro*. Cell *33*, 509–518.
9. Zamore, P.D., and Green, M.R. (1989). Identification, purification, and biochemical characterization of U2 small nuclear ribonucleoprotein auxiliary factor. Proc. Natl. Acad. Sci. USA *86*, 9243–9247.
10. Ruskin, B., Zamore, P.D., and Green, M.R. (1988). A factor, U2AF, is required for U2 snRNP binding and splicing complex assembly. Cell *52*, 207–219.

11. Buratti, E., and Baralle, F.E. (2004). Influence of RNA secondary structure on the pre-mRNA splicing process. Mol. Cell Biol. *24*, 10505–10514.

12. Havens, M.A., and Hastings, M.L. (2016). Splice-switching antisense oligonucleotides as therapeutic drugs. Nucleic Acids Res. *44*, 6549–6563.

13. Shibata, S., Ajiro, M., and Hagiwara, M. (2020). Mechanism-Based Personalized Medicine for Cystic Fibrosis by Suppressing Pseudo Exon Inclusion. Cell Chem. Biol. *27*, 1472–1482.e6.

14. Nishida, A., Kataoka, N., Takeshima, Y., Yagi, M., Awano, H., Ota, M., Itoh, K., Hagiwara, M., and Matsuo, M. (2011). Chemical treatment enhances skipping of a mutated exon in the dystrophin gene. Nat. Commun. *2*, 308.

15. Sako, Y., Ninomiya, K., Okuno, Y., Toyomoto, M., Nishida, A., Koike, Y., Ohe, K., Kii, I., Yoshida, S., Hashimoto, N., et al. (2017). Development of an orally available inhibitor of CLK1 for skipping a mutated dystrophin exon in Duchenne muscular dystrophy. Sci. Rep. *7*, 46126.

16. Boisson, B., Honda, Y., Ajiro, M., Bustamante, J., Bendavid, M., Gennery, A.R., Kawasaki, Y., Ichishima, J., Osawa, M., Nihira, H., et al. (2019). Rescue of recurrent deep intronic mutation underlying cell type-dependent quantitative NEMO deficiency. J. Clin. Invest. *129*, 583–597.

17. Wu, G., Fan, L., Edmonson, M.N., Shaw, T., Boggs, K., Easton, J., Rusch, M.C., Webb, T.R., Zhang, J., and Potter, P.M. (2018). Inhibition of SF3B1 by molecules targeting the spliceosome results in massive aberrant exon skipping. RNA *24*, 1056–1066.

18. Muraki, M., Ohkawara, B., Hosoya, T., Onogi, H., Koizumi, J., Koizumi, T., Sumi, K., Yomoda, J.i., Murray, M.V., Kimura, H., et al. (2004). Manipulation of alternative splicing by a newly developed inhibitor of Clks. J. Biol. Chem. *279*, 24246–24254.

19. Yoshida, M., Kataoka, N., Miyauchi, K., Ohe, K., Iida, K., Yoshida, S., Nojima, T., Okuno, Y., Onogi, H., Usui, T., et al. (2015). Rectifier of aberrant mRNA splicing recovers tRNA modification in familial dysautonomia. Proc. Natl. Acad. Sci. USA *112*, 2764–2769.

20. Kotake, Y., Sagane, K., Owa, T., Mimori-Kiyosue, Y., Shimizu, H., Uesugi, M., Ishihama, Y., Iwata, M., and Mizui, Y. (2007). Splicing factor SF3b as a target of the antitumor natural product pladienolide. Nat. Chem. Biol. *3*, 570–575.

21. Hasegawa, M., Miura, T., Kuzuya, K., Inoue, A., Won Ki, S., Horinouchi, S., Yoshida, T., Kunoh, T., Koseki, K., Mino, K., et al. (2011). Identification of SAP155 as the target of GEX1A (Herboxidiene), an antitumor natural product. ACS Chem. Biol. *6*, 229–233.

22. Kaida, D., Motoyoshi, H., Tashiro, E., Nojima, T., Hagiwara, M., Ishigami, K., Watanabe, H., Kitahara, T., Yoshida, T., Nakajima, H., et al. (2007). Spliceostatin A targets SF3b and inhibits both splicing and nuclear retention of pre-mRNA. Nat. Chem. Biol. *3*, 576–583.

23. Ling, Y., Alshareef, S., Butt, H., Lozano-Juste, J., Li, L., Galal, A.A., Moustafa, A., Momin, A.A., Tashkandi, M., Richardson, D.N., et al. (2017). Pre-mRNA splicing repression triggers abiotic stress signaling in plants. Plant J. *89*, 291–309.

24. Signal, B., Gloss, B.S., Dinger, M.E., and Mercer, T.R. (2018). Machine learning annotation of human branchpoints. Bioinformatics *34*, 920–927.

25. Corvelo, A., Hallegger, M., Smith, C.W.J., and Eyras, E. (2010). Genome-wide association between branch point properties and alternative splicing. PLoS Comput. Biol. *6*, e1001016.

26. Mercer, T.R., Clark, M.B., Andersen, S.B., Brunck, M.E., Haerty, W., Crawford, J., Taft, R.J., Nielsen, L.K., Dinger, M.E., and Mattick, J.S. (2015). Genome-wide discovery of human splicing branchpoints. Genome Res. *25*, 290–303.

27. Taniguchi-Ikeda, M., Kobayashi, K., Kanagawa, M., Yu, C.C., Mori, K., Oda, T., Kuga, A., Kurahashi, H., Akman, H.O., DiMauro, S., et al. (2011). Pathogenic exon-trapping by SVA retrotransposon and rescue in Fukuyama muscular dystrophy. Nature *478*, 127–131.

28. Canson, D., Glubb, D., and Spurdle, A.B. (2020). Variant effect on splicing regulatory elements, branchpoint usage, and pseudoexonization: Strategies to enhance bioinformatic prediction using hereditary cancer genes as exemplars. Hum. Mutat. *41*, 1705–1721.

29. Nazari, I., Tayara, H., and Chong, K.T. (2019). Branch Point Selection in RNA Splicing Using Deep Learning. IEEE Access *7*, 1800–1807.

30. Mendell, J.R., Rodino-Klapac, L.R., Sahenk, Z., Roush, K., Bird, L., Lowes, L.P., Alfano, L., Gomez, A.M., Lewis, S., Kota, J., et al.; Eteplirsen Study Group (2013). Eteplirsen for the treatment of Duchenne muscular dystrophy. Ann. Neurol. *74*, 637–647.

31. Frank, D.E., Schnell, F.J., Akana, C., El-Husayni, S.H., Desjardins, C.A., Morgan, J., Charleston, J.S., Sardone, V., Domingos, J., Dickson, G., et al.; SKIP-NMD Study Group (2020). Increased dystrophin production with golodirsen in patients with Duchenne muscular dystrophy. Neurology *94*, e2270–e2282.

32. Komaki, H., Nagata, T., Saito, T., Masuda, S., Takeshita, E., Sasaki, M., Tachimori, H., Nakamura, H., Aoki, Y., and Takeda, S. (2018). Systemic administration of the antisense oligonucleotide NS-065/NCNP-01 for skipping of exon 53 in patients with Duchenne muscular dystrophy. Sci. Transl. Med. *10*, eaan0713.

33. Wagner, K.R., Kuntz, N.L., Koenig, E., East, L., Upadhyay, S., Han, B., and Shieh, P.B. (2021). Safety, tolerability, and pharmacokinetics of casimersen in patients with Duchenne muscular dystrophy amenable to exon 45 skipping: A randomized, double-blind, placebo-controlled, dose-titration trial. Muscle Nerve *64*, 285–292.

34. Holgersen, E.M., Gandhi, S., Zhou, Y., Kim, J., Vaz, B., Bogojeski, J., Bugno, M., Shalev, Z., Cheung-Ong, K., Gonçalves, J., et al. (2021). Transcriptome-Wide Off-Target Effects of Steric-Blocking Oligonucleotides. Nucleic Acid Ther. *31*, 392–403.

35. Watanabe, N., Nagata, T., Satou, Y., Masuda, S., Saito, T., Kitagawa, H., Komaki, H., Takagaki, K., and Takeda, S. (2018). NS-065/NCNP-01: An Antisense Oligonucleotide for Potential Treatment of Exon 53 Skipping in Duchenne Muscular Dystrophy. Mol. Ther. Nucleic Acids *13*, 442–449.

36. Takeuchi, A., Takahashi, Y., Iida, K., Hosokawa, M., Irie, K., Ito, M., Brown, J.B., Ohno, K., Nakashima, K., and Hagiwara, M. (2020). Identification of Qk as a Glial Precursor Cell Marker that Governs the Fate Specification of Neural Stem Cells to a Glial Cell Lineage. Stem Cell Rep. *15*, 883–897.